DOI 10.1515/hf-2012-0120 — Holzforschung 2013; 67(4): 463–471

Li-Ting Ma, Sheng-Yang Wang, Yen-Hsueh Tseng, Yi-Ru Lee and Fang-Hua Chu*

Cloning and characterization of a 2,3-oxidosqualene cyclase from *Eleutherococcus trifoliatus*

Abstract: The 2,3-oxidosqualene cyclases (OSCs) are a family of enzymes that have an important role in plant triterpene biosynthesis. In this study, an OSC gene designed *EtLUS* from *Eleutherococcus trifoliatus* has been cloned. *EtLUS* includes a 2292-bp open reading frame and encodes a 763-amino acid protein. *Et*LUS has an MLCYCR motif, which is conserved in lupeol synthases. Comparison of active-site residues and gene expression in yeast showed that *Et*LUS synthesizes lupeol. However, *Et*LUS has the highest sequence identity with β-amyrin synthases from Araliaceae rather than lupeol synthases, adding new perspective to the evolution of the OSCs of Araliaceae. Furthermore, *EtLUS* is upregulated in leaf tissues under methyl jasmonate treatment, which can be interpreted that lupeol and its derivatives play an ecological and physiological role in plant defense against pathogens and insect herbivores.

Keywords: Araliaceae, *Eleutherococcus trifoliatus*, lupeol, methyl jasmonate, 2,3-oxidosqualene cyclase

***Corresponding author: Fang-Hua Chu,** School of Forestry and Resource Conservation, National Taiwan University, Taipei 10617, Taiwan, e-mail: fhchu@ntu.edu.tw
Li-Ting Ma and Yi-Ru Lee: School of Forestry and Resource Conservation, National Taiwan University, Taipei 10617, Taiwan
Sheng-Yang Wang and Yen-Hsueh Tseng: Department of Forestry, National Chung-Hsing University, Taichung 40227, Taiwan

Introduction

Eleutherococcus trifoliatus (L.) S.Y. Hu var. *trifoliatus* (=*Acanthopanax trifoliatus*, Araliaceae) is a shrub with ternately compound leaves. It is used in folk medicine in Vietnam, Taiwan, and China for bruising, neuralgia, impotence, and gout because of its ginseng-like activity (Lischewski et al. 1985; Ohashi 1993; Yook et al. 1999). Many studies have reported the secondary metabolic bioactivities of compounds from the Araliaceae. Triterpenes such as ginsenoside and ciwujianosides isolated from *Panax* species and *Eleutherococcus senticosus*, respectively, are among the most commonly reported. Some compounds from this family have been found to possess important pharmacological activities, including anti-inflammatory, anti-cancer, anti-amnestic, and anti-aging effect, which led to an increased interest in this group of plants (Kenarova et al. 1990; Mochizuki et al. 1995; Shinkai et al. 1996; Jung et al. 2003; Cheng et al. 2005; Seo et al. 2005).

Terpene compounds have a plenty of bioactivities. Trapp and Croteau (2001) summarized the genomic organization of plant terpene synthases, and in many cases, typical terpene synthases were identified and characterized, such an α-pinene synthase (Chu et al. 2009), β-cadinene synthase (Kuo et al. 2012), or a sesquiterpene synthase (Wen et al. 2012), to mention a few. Triterpenes are a large subgroup of the terpene superfamily (Xu et al. 2004), which are biosynthesized directly from 2,3-oxidosqualene by an enzyme family named the 2,3-oxidosqualene cyclases (OSCs) (Segura et al. 2003). Different OSCs have different product specificities that can be divided into sterol precursors and triterpene alcohols; the OSCs can thus be considered a critical branch point between primary and secondary metabolism and a critical point in the generation of triterpene skeletal diversity (Phillips et al. 2006).

In recent years, a number of triterpene synthases have been cloned and characterized from various plant species; those articles contributed to a better understanding the biosynthesis of plant triterpenes (Basyuni et al. 2006; Guhling et al. 2006). Some triterpene compounds are thought to participate in plant defense systems because of the anti-microbial, fungicidal, and insecticidal activities (Mylona et al. 2008). Multiple pharmacological activities have also been observed. Glycyrrhizin is a triterpene compound that exists in the roots and stolons of *Glycyrrhiza* plants and may be suitable for the treatment of liver diseases and allergic diseases (Hayashi and Sudo 2007). *Panax ginseng* contains unique triterpene compounds named ginsenosides. Each ginsenoside has been shown to have different pharmacological effects, supporting its traditional use as a medical plant (Liang and Zhao 2008).

To date, five triterpenoid carboxylic acids and three lupane-glycosides have been reported in *E. trifoliatus* (Ty et al. 1984, 1985; Lischewski et al. 1985; Yook et al.

1999). However, the biosynthesis pathways of triterpene compounds in this plant remain unknown. In the present study, a gene involved in triterpene biosynthesis in *E. trifoliatus* should be identified and characterized. To understand the physiology functions and properties of this gene, its expression will be analyzed in different tissues and under treatment conditions with an elicitor, namely with methyl jasmonate (MeJA).

Materials and methods

Plant materials and culture conditions

Plants were collected from a field on the Chiufenershan Mountain in Nantou County of Taiwan. The plants were incubated under greenhouse conditions at 25°C with natural light. The plant tissue was harvested and frozen instantaneously in liquid N_2. The tissues were stored at -80°C in advance for RNA preparation. Yeast strain GIL77 (*gal2 hem3-6 erg7 ura3167*) was selected as the host for gene expression, maintained on YPD medium (1% yeast extract, 2% peptone, 2% dextrose) supplemented with hemin (13 μg ml^{-1}), ergosterol (20 μg ml^{-1}), and Tween 80 (5 mg ml^{-1}).

Cloning of OSC cDNA

Fresh leaf tissue was weighed and ground to a fine powder under liquid N_2, and total RNA isolation was performed by Plant Total RNA Miniprep Purification Kit (Hopegen, Taichung, Taiwan). Total RNA (2 μg) was reverse-transcribed with SuperScript™ III reverse transcriptase (Invitrogen, Carlsbad, CA, USA) according to the manufacturer's protocol. The core sequence was amplified by degenerate primers triTPS1F (CAATGGA(G/T)CA(C/T)(A/G)TTCATTATGA) and triTPS4R (TCCT(C/G)(C/T)TGAGGAAA(A/G)TCACC), which was based on highly conserved region on the alignment of published sequences of OSC. The 3′- and 5′-end amplification of cDNA were carried out with 3′- and 5′-RACE System (Invitrogen, Carlsbad, CA, USA), respectively. All specific primers were based on the sequence of core fragment. Protein structure was predicted by Swiss-Model Repository (http://swissmodel.expasy.org) and visualized by the Chimera program (Resource for Biocomputing, Visualization, and Informatics at the University of California, San Francisco, CA, USA) (Pettersen et al. 2004).

Sequences alignment and phylogenetic analyses were based on the neighbor-joining method and using the ClustalW website and the MEGA5.0 software (http://www.megasoftware.net/). The phylogenetic tree was built based on 1000 bootstrap replications. All the sequences of this analysis are described in Table 1.

Functional expression of OSC cDNA in yeast and analysis of triterpene products

The full-length cDNA of *EtLUS* was obtained by a forward primer with a *Sac*I site (5′-CGAGCTC-ATG TGG AAG CTG AAG ATA GCC GAA GGA G-3′) and a reverse primer with a *Not*I site (5′-ATAGTTTAGCG-GCCG-TTA GGC ACC TAG GGT CGG TAA TGG TAC-3′). PCR was performed by Phusion® High-Fidelity DNA Polymerase (Finnzyme, Espo, Finland). The PCR amplification program was designed as follows: one cycle of initial denaturation at 98°C for 30 s, 30 cycles at 98°C for 17 s, 60°C for 15 s, and 72°C for 60 s, and finally, 72°C for 10 min.

The full-length PCR product was digested with *Sac*I and *Not*I restriction enzymes (New Rngland Biolabs, Hitchin, UK), and ligated into yeast expression vector pYES2 (Invitrogen, Carlsbad, CA, USA) derived from *GAL1* promoter with T4 DNA ligase (Promega, Heidelberg, Germany). The plasmid was transformed into yeast mutant GIL77 by electroporation. The transformed yeast was inoculated in 30 ml synthetic complete medium without uracil (SC-Ura) and containing hemin (13 μg ml^{-1}), ergosterol (20 μg ml^{-1}), and Tween 80 (5 mg ml^{-1}), incubated at 30°C for 2 days, and then transferred to a new SC-Ura medium supplemented with 2% galactose for glucose. After induction of galactose and the stabilization of incubation for 24 h in 0.1 M potassium phosphate buffer (pH 7.0) supplemented with 3% glucose and hemin, cells were collected by centrifugation at 1750 *g* for 5 min and refluxed with 5 ml 20% KOH/50% ethanol at 90°C for 10 min and extracted twice with 5 ml hexane. The solvent was dried out by a gentle stream of N_2 and redissolved in 1 ml hexane.

The final extract was analyzed by TLC that was developed with hexane/ethyl acetate (9:1, v/v) and then visualized by 5% phosphomolybdic acid in ethanol. To identify the chemical structures, the extracts were directly derivatized with bis-N,N-(trimethylsilyl)- trifluoroacetamide (BSTFA) in pyridine (30 min at 70°C). The product analysis was observed using an ITQ 900TM GC/MS instrument (Thermo Scientific, Dreieich, Germany) and a DB-5 capillary column (30×0.25 mm i.d., 0.25 μm film thickness; J&W Scientific, Folsom, CA, USA). For the temperature program, injection was done at 110°C and held constant for 1 min (He at 1 ml min^{-1}), then increased to 260°C (40°C min^{-1}) and held constant for 5 min, and then further increased to 290°C (5°C min^{-1}) and held for 10 min.

Expression analysis of *Et*LUS in *E. trifoliatus* organs and MeJA treatment

Unexpanded leaves, mature leaves, shoots, stems, roots, and fruits were collected from plants. Total RNA was extracted from powder with TRIzol® reagent (Invitrogen, Carlsbad, CA, USA), then cDNA was synthesized as described previously. The nucleotide sequences of the gene specific primers were as follows: 2osc3R2 (5′-GTT ATA TCC TGG GCA CCG AAA GAA GGA G-3′) and 2oscR (5′-ACC GAC CCT AGG TGC CTA AAT AGC-3′). Actin as internal control was amplified using the primer sets: actin-F (5′-GCC ATC CTT CGT CTT GAC CTT GCT G-3′) and actin-R (5′-CTG TTG GAA GGT GCT GAG GGA TGC-3′). To eliminate the amplification of homologous transcripts, two primers sets were designed in the coding region and the 3′-UTR, respectively. PCR amplification was carried out with initial denaturation at 94°C for 3 min, 25 cycles each at 94°C for 30 s, 60°C for 30 s, and 72°C for 30 s, and finally, 72°C for 60 s.

For MeJA treatment, plants were sprayed with 10 mM MeJA solution until totally wet and placed alone in the plant growth incubator. Leaves were harvested as samples after 6, 12, 24, and 48 h, and RNA extraction and RT-PCR were carried out as described previously.

GenBank accession	Function	Species
β-Amyrin synthase		
BAG82628	β-Amyrin synthase	*Ara. thaliana*
BAA97558	β-Amyrin synthase	*Pisum sativum*
ACV21067	β-Amyrin synthase	*Glycyrrhiza uralensis*
BAE53429	β-Amyrin synthase	*Lotus japonicus*
AAO33580	Multifunctional β-Amyrin synthase	*L. japonicus*
ABL07607	β-Amyrin synthase	*Polygala tenuifolia*
ABK76265	β-Amyrin synthase	*Vaccaria hispanica*
BAE43642	β-Amyrin synthase	*Euphorbia tirucalli*
BAF80443	β-Amyrin synthase	*Bruguiera gymnorhiza*
BAB83088	β-Amyrin synthase	*Betula platyphylla*
ADU52574	β-Amyrin synthase	*Solanum lycopersicum*
AAS83468	β-Amyrin synthase	*Bupleurum kaoi*
BAA33461	β-Amyrin synthase	*P. ginseng*
ACA13386	β-Amyrin synthase	*Artemisia annua*
ADK12003	β-Amyrin synthase	*A. elata*
BAA33722	β-Amyrin synthase	*P. ginseng*
Lupeol synthase		
ADK35126	Lupeol synthase	*K. daigremontiana*
AAD05032	Lupeol synthase	*Ara. thaliana*
ABB76766	Lupeol synthase	*R. communis*
BAF80444	Lupeol synthase	*B. gymnorhiza*
BAA86930	Lupeol synthase	*O. europaea*
BAA86932	Lupeol synthase	*Taraxacum officinale*
BAB83087	Lupeol synthase	*Bet. platyphylla*
BAD08587	Lupeol synthase	*Glycyrrhiza glabra*
Lanosterol synthase		
NP_190099	Lanosterol synthase	*Ara. thaliana*
Cycloartenol synthase		
CAM91422	Cycloartenol synthase	*Dioscorea zingiberensis*
AAC04931	Cycloartenol synthase	*Ara. thaliana*
ADK35127	Cycloartenol synthase	*K. daigremontiana*
ACA28830	Cycloartenol synthase	*S. lycopersicum*
ABB76767	Cycloartenol synthase	*R. communis*
BAF73929	Cycloartenol synthase	*Rhizophora stylosa*
BAA76902	Cycloartenol synthase	*G. glabra*
BAB83086	Cycloartenol synthase	*Bet. platyphylla*
ABY60426	Cycloartenol synthase	*Panax notoginseng*
BAA33460	Cycloartenol synthase	*P. ginseng*
AAS01524	Cycloartenol synthase	*Centella asiatica*

Table 1 Amino acid sequences used in phylogenetic analysis.

Results

Characterization of the encoding OSC in *E. trifoliatus*

In previous studies of *E. trifoliatus*, triterpene compounds were isolated mainly from leaves; in the present study, cDNA from leaves was used to clone OSCs. A full-length sequence named *EtLUS* (GenBank accession no. JQ087376) was obtained using PCR amplification with degenerated primers and the RACE method. The open reading frame of *EtLUS* is 2292 bp and encodes a 763-amino acid protein with a molecular weight of 87 kDa. It contains four QW motifs that are thought to contribute to the fold stability of the protein (Wendt et al. 1997) and the OSC family-conserved substrate-binding site DCTAE (Figure 1).

Active catalytic residue identification has been the focus of study of OSCs, and it has been proved that the MLCYCR and MWCYCR motifs are critical in the product specificities of lupeol and β-amyrin synthase, respectively (Kushiro et al. 2000). The alignment of the amino

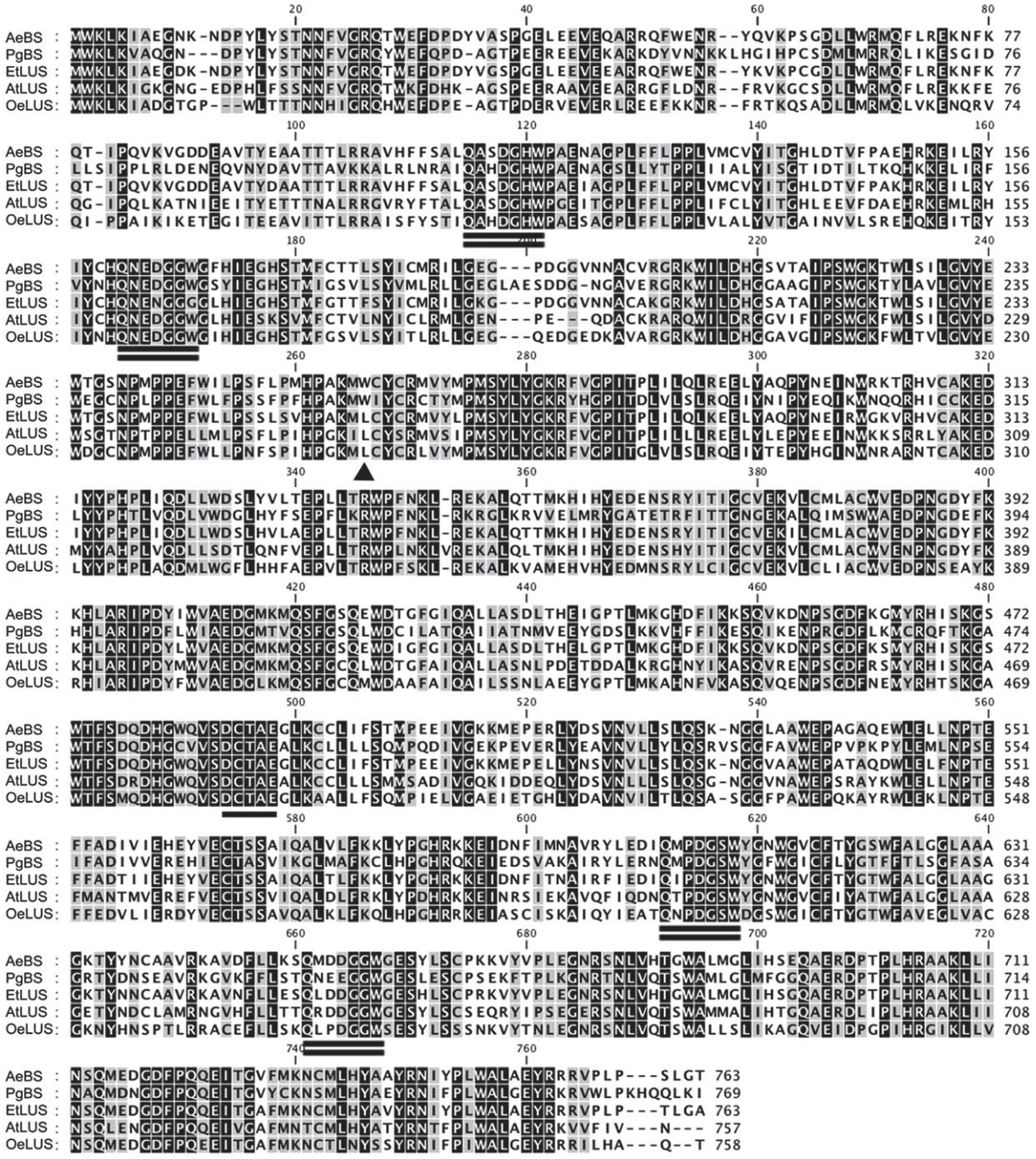

Figure 1 Alignment of amino acid sequences of *Et*LUS and four related β-amyrin synthases and lupeol synthases. AeBS is a β-amyrin synthase from *A. elata* (ADK12003). PgBS is a β-amyrin synthase from *P. ginseng* (BAA33722). AtLS1 is a lupeol synthase from *Ara. thaliana* (AAD05032). OeLS is a lupeol synthase from *O. europaea* (BAA86930). The DCTAE motif is underlined with a black line, and the four QW motifs are marked using double black lines. The ML(W)CYCR motif is marked using black triangles.

acid sequence of *Et*LUS and other characterized OSCs shows that *Et*LUS has the same active catalytic residue (Leu259 in the MLCYCR motif) as lupeol synthase but with a different active catalytic residue from β-amyrin synthase (Figure 1).

The protein structure predicted by Swiss-Model Workplace is aligned with a human lanosterol synthase (1W6JA) that is also an OSC (Thoma et al. 2004). Between these two domains, *EtLUS* has a large active-site cavity that the DCTAE motif approaches, and this domain is located at amino acids 486–490 (Figure 2a). On the basis of the structure of human OSC proved by Thoma et al. (2004), we postulate that Asp486 pronates the epoxide group of 2,3-oxidosqualene to initiate cyclization of OSC,

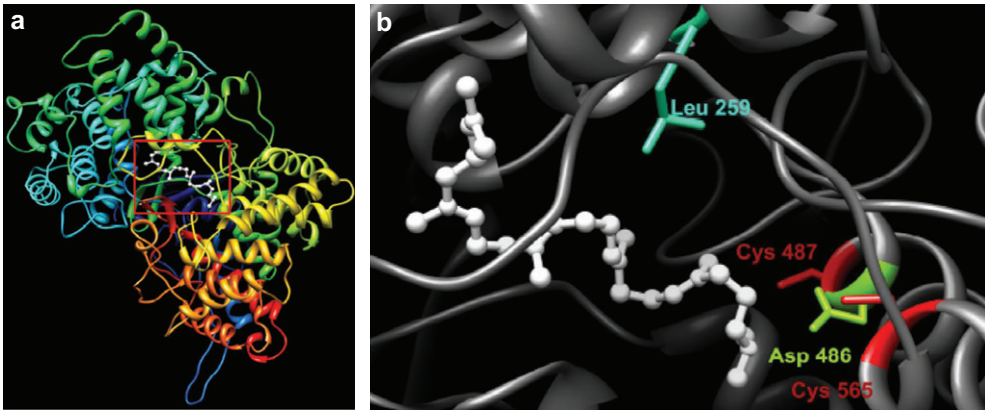

Figure 2 Protein structure prediction and active site of *Et*LUS. (a) The whole *Et*LUS structure with the active site in the center (red frame) in which the substrate, 2,3-oxidosqualene (white) is catalyzed. (b) The relative positions of substrate-binding residue Asp486 (green), the active catalytic residue Leu259 (blue), hydrogen-bonding partners Cys487 and Cys565 (red), and 2,3-oxidosqualene (white).

and hydrogen-bonding partners with Asp486 were also found in Cys487 and Cys565 (Figure 2b).

Functional expression of OSC in yeast

To further identify the function of *Et*LUS, functional expression of the cloned gene was attempted. *EtLUS* cDNA was ligated into the vector pYES2 and expressed under the control of the *GAL1* promoter in yeast mutant GIL77, which lacks lanosterol synthase activity, to decrease the competition for the substrate of OSC, 2,3-oxidosqualene. Because of this deficiency, exogenous ergosterol, which is derived from lanosterol, is essential for cell growth. The empty vector was also transformed into GIL77 as a negative control.

Lipid extract and authentic standards were applied to TLC plates. The gene expression of *EtLUS* in GIL77 resulted in a product with the same mobility as lupeol (Figure 3a) and β-amyrin (data not shown). Both transformants (pYES2 and pYES2-*EtLUS*) had the same signal, which was possibly ergosterol. To identify the chemical structure of each signal in the TLC plates, the extracts were analyzed by GC/MS. Comparison of the MS fragmentation patterns of authentic triterpene compounds such as β-amyrin, lupeol, cycloartenol, and ergosterol showed that two transformants contained ergosterol, in agreement with the results of TLC. In addition, the extracts from yeast harboring *EtLUS* cDNA comprised one major compound, which showed at 21.7 min and was consistent with the retention time of the lupeol standard (Figure 3b). To elucidate the structure, MS characteristics were compared with the lupeol standard, revealing fraction peaks at *m*/*z* 189, 218, and

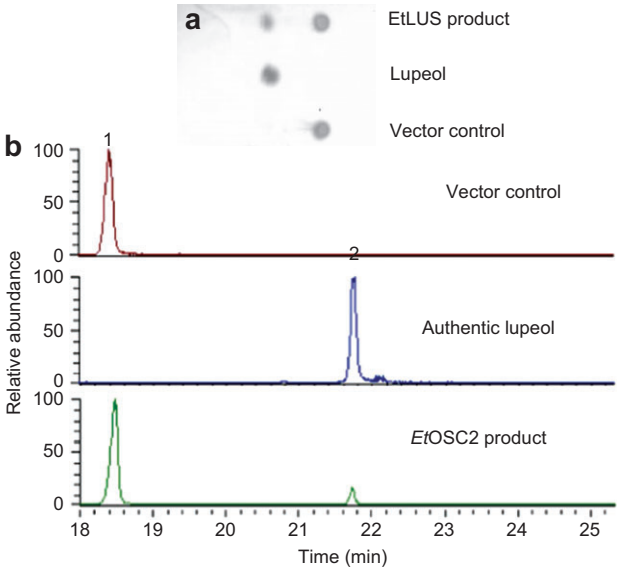

Figure 3 Chromatographic analysis of the hexane extract from yeast and authentic lupeol as standard. (a) Comparison patterns of TLC patterns of yeast transformed with pYES2 (vector control) and pYES2-*Et*LUS (*Et*LUS product). (b) GC analysis of three extracts: compound 1 (ergosterol) and compound 2 (lupeol). The mass spectrum of compound 2 is shown in Figure 4.

498, which were also identical to the lupeol standard (Figure 4).

Expression of *Et*LUS in *E. trifoliatus* organs and MeJA treatment

RT-PCR was performed to examine the expression of *EtLUS* in different tissues of *E. trifoliatus*. The accumulation of *EtLUS* transcripts was observed in all leaf tissues

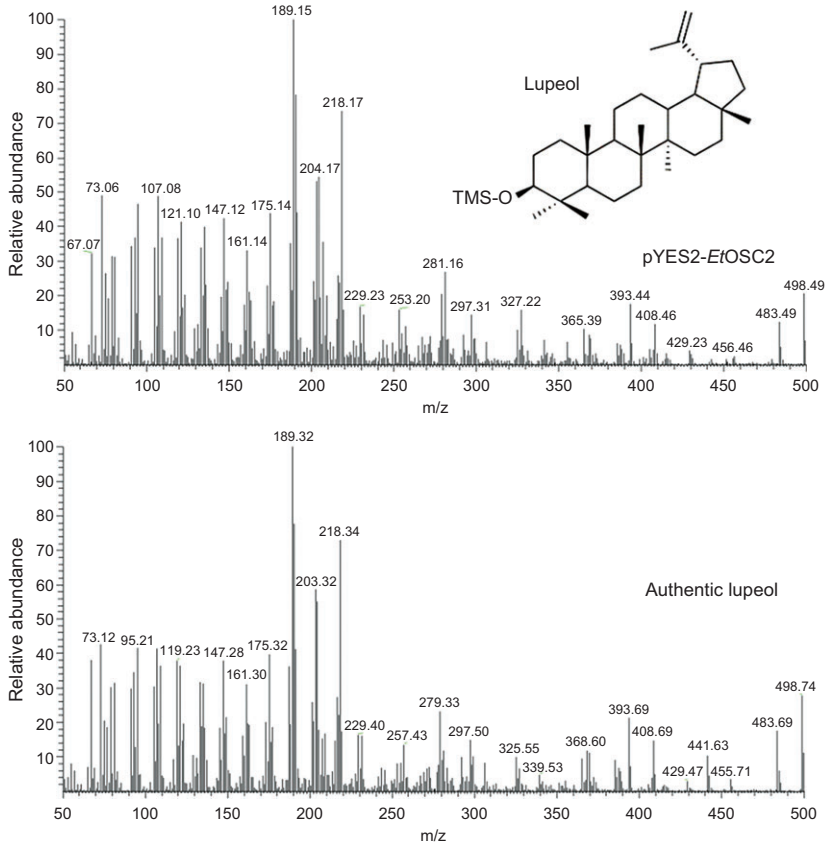

Figure 4 Mass spectra of compound 2 in yeast (pYES2-*EtLUS*) and lupeol standard. After derivation with BSTFA, lupeol was transformed into trimethylsilyl (TMS) derivatives and showed a peak at *m*/*z* 498 corresponding to the parent ion.

and young stems (Figure 5a). Meanwhile, few *EtLUS* transcripts were detected in root tissues, and none of them in woody stems and fruits. After MeJA treatment, the expression of *EtLUS* from mature leaves increased continuously from 6 h to 2 days after treatment (Figure 5b). These results show that *EtLUS* could be induced by MeJA and thus might be related to plant defense.

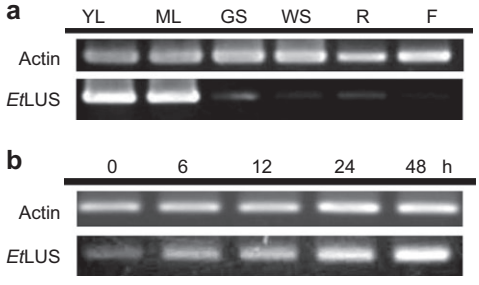

Figure 5 RT-PCR analysis of expression levels of *Et*LUS.
(a) Expression patterns in different plant organs (YL, young leaves; ML, mature leaves; GS, green shoots; WS, woody shoots; R, roots; F, fruits). (b) Expression pattern after exposure to 10 mM MeJA for 0, 6, 12, 24, and 48 h.

Discussion and conclusions

According to the phylogenetic analysis of *Et*LUS and 41 other previously characterized plant OSCs (Table 1), they are separated into three groups: cycloartenol synthases, β-amyrin synthases, and lupeol synthases (Figure 6). The amino acid sequence of *Et*LUS exhibits 90–92% sequence identity with β-amyrin synthase from *P. ginseng* (GenBank accession no. BAA33461) and *Aralia elata* (GenBank accession no. ADK12003), which belong to the same family as *E. trifoliatus* and has a 72–76% identity with lupeol synthase from *Ricinus communis* (GenBank accession no. ABB76766) and *Kalanchoe daigremontiana* (GenBank accession no. ADK35126).

Alhough *Et*LUS shares the highest degree of sequence identity with β-amyrin synthase (92%) based on phylogenetic tree analysis, GC/MS analysis revealed that it encodes a lupeol synthase. In fact, β-amyrin and lupeol synthases fold the substrate into the same pre-*chair-chair-chair* conformation. Continuously, lupeol synthase turns the dammarenyl cation into lupeol through an intermediate named lupenyl cation; β-amyrin synthase forms

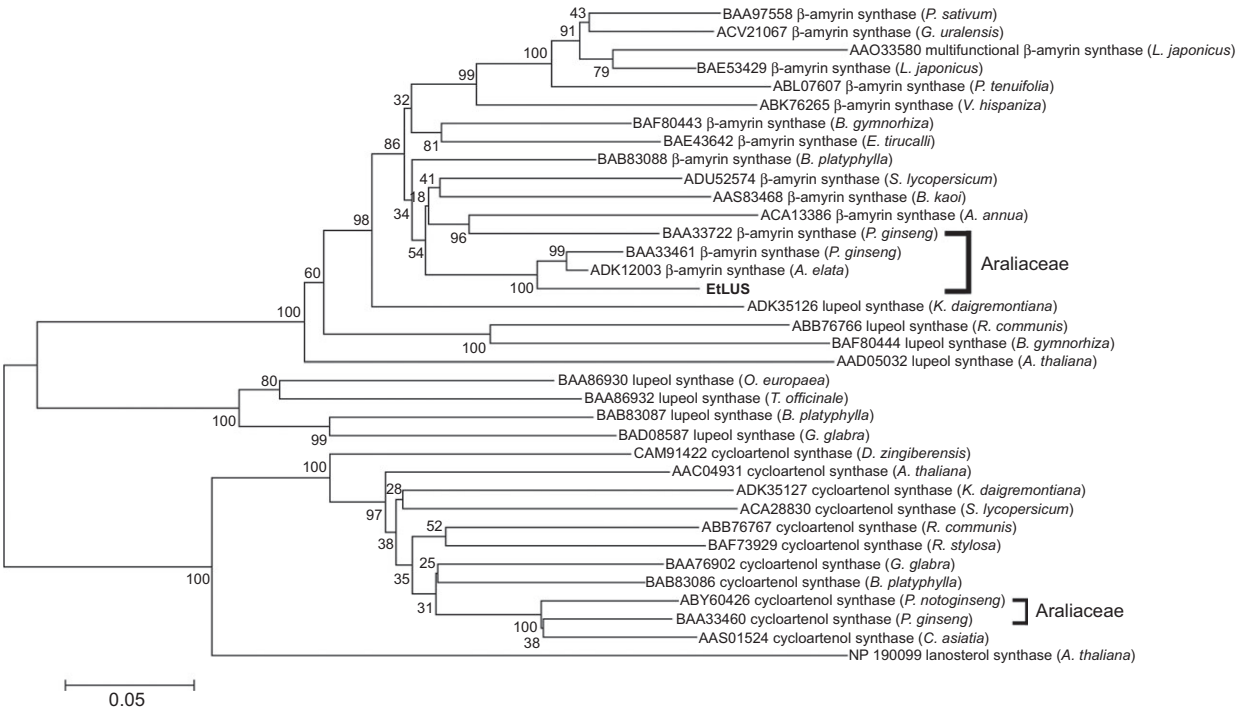

Figure 6 Phylogenetic analysis contrasting EtLUS with characteristic OSCs from other plant species. Scale bar represents 0.05 amino acid substitutions per site. Numbers show bootstrap values from 1000 replicates. The GenBank accession numbers used in this analysis are presented in Table 1.

the two intermediates, lupenyl cation and oleanyl cation (Segura et al. 2003), which means that there is an additional step in β-amyrin synthase cyclization.

The difference in active catalytic residue is a major reason for the diversity of the OSCs (Segura et al. 2003). Some active catalytic residues have been described in reports of site-directed mutagenesis and X-ray crystal structure of these proteins (Kushiro et al. 2000). Two such sites are MWCYCR of β-amyrin synthase PNY from *P. ginseng* and MLCYCR of lupeol synthase OEW from *Olea europaea*. These sites might control product specificity by a series of gene mutagenesis and functional expression in yeast (Kushiro et al. 2000; Segura et al. 2003). Compared with the protein structure of EtLUS, the key residue (Leu) of MLCYCR is located on the side of the catalytic cavity and catalyzes the cyclization of lupeol (Figure 2b) (Thoma et al. 2004). In addition, lupeol synthase from *R. communis* (RcLUS) and *K. daigremontiana* (KdLUS), which share the highest identity with *Et*LUS in the lupeol synthase group, contain MFCYCR and MWCYCR, respectively (data not shown). The substitution of Leu with Phe in the OEW motif did not cause a change in lupeol synthesis. However, KdLUS is known to be bifunctional, synthesizing both lupeol and β-amyrin, which may be caused by the MWCYCR motif. Our results show that EtLUS is located in a transitional area of phylogenetic tree between lupeol synthase and β-amyrin synthase.

In the evolution of the Araliaceae, *Eleutherococcus* was thought to be a paraphyletic group that derived *Aralia* and *Panax* (Wen et al. 2001). This relationship is similar to the relationship between lupeol synthase and β-amyrin synthase, and the high identity between triterpene synthases from the Araliaceae can be interpreted that *Et*LUS could be an ancestor of β-amyrin synthase in *A. elata* and *P. ginseng*. However, *Et*LUS is the first lupeol synthase studied in Araliaceae, and genome-wide analysis is needed to elucidate the evolution of triterpene synthases in this plant family.

Since the first lupeol synthase (LS) in *Arabidopsis thaliana* was reported (Herrera et al. 1998), much attention has been paid to its function in plant physiology centering on its nodule formation (Iturbe-Ormaetxe et al. 2003; Hayashi et al. 2004; Delis et al. 2011). In castor beans, lupeol synthase is responsible for the formation of the epicuticular crystals on the surface of the stem, which can cause mechanical impediment to the attachment of herbivores (Guhling et al. 2006). Under natural conditions, insect wounding and necrotrophic pathogens induce the jasmonate (JA) response (McConn et al. 1997; Thaler et al. 2004), and then secondary metabolites accumulate in

defense (Pauwels et al. 2009). In metabolic engineering, elicitors such as JA can be exploited to increase the production of bioactive compounds, such as the triterpene saponins in *Medicago truncatula* (Suzuki et al. 2005). JA is frequently favored as an elicitor because of the wide variety of effective secondary metabolites that it can upregulate (Pauwels et al. 2009). In the present study, an increased response of *EtLUS* transcripts after MeJA treatment in leaves of *E. trifoliatus* could be verified. Accordingly, lupeol and its derivatives might be involved in the defense against plant pathogens and insect herbivores.

Many lupeol derivatives have been identified from the leaves of *E. trifoliatus*, including acantrifoic acid A, lupane-triterpene carboxylic acids, and acantrifosides A, B, and C (Ty et al. 1984, 1985; Lischewski et al. 1985; Yook et al. 1999; Kiem et al. 2003; Liem et al. 2003). Lupeol is a pentacyclic triterpene that has many important pharmacological activities, including inflammation reduction, angiogenesis inhibition, and tumor inhibition (Fernández et al. 2001; You et al. 2003; Saleem et al. 2004; Prasad et al. 2008). In drug synthesis, lupeol is useful because its derivatives can be developed to improve curative effects (Reddy et al. 2009). In the present study, *Et*LUS from leaves of *E. trifoliatus* could be characterized, and a method is provided for lupeol production *in vitro*. However, further work is needed to understand the role of lupeol in physiological mechanisms and the direction of evolution of the whole OSC family.

Acknowledgment: Financial assistance from the Council of Agriculture Executive Yuan is gratefully acknowledged.

Received July 17, 2012; accepted October 22, 2012; previously published online November 23, 2012

References

Basyuni, M., Oku, H., Inafuku, M., Baba, S., Iwasaki, H., Oshiro, K., Okabe, T., Shibuya, M., Ebizuka, Y. (2006) Molecular cloning and function expression of a multifunctional triterpene synthase cDNA from a mangrove species *Kandelia candel* (L.) Druce. Phytochemistry 67:2517–2524.

Cheng, Y., Shen, L.H., Zhang, J.T. (2005) Anti-amnestic and anti-aging effects of ginsenoside Rg1 and Rb1 and its mechanism of action. Acta Pharmacol Sin. 26:143–149.

Chu, F.H., Kuo, P.M., Chen, Y.R., Wang, S.Y. (2009) Cloning and characterization of α-pinene synthase from *Chamaecyparis formosensis* Matsum. Holzforschung 63:69–74.

Delis, C., Krokida, A., Georgiou, S., Peña-Rodriguez, L.M., Kavroulakis, N., Ioannou, E., Roussis, V.A., Osbourn, E., Papadopoulou, K. (2011) Role of lupeol synthase in *Lotus japonicus* nodule formation. New Phytol. 189:335–346.

Fernández, M.A., de las Heras, B., Garcia, M.D., Sáenz, M.T., Villar, A. (2001) New insights into the mechanism of action of the anti-inflammatory triterpene lupeol. J. Pharm. Pharmacol. 53:1533–1539.

Guhling, O., Hobl, B., Yeats, T., Jetter, R. (2006) Cloning and characterization of lupeol synthase involved in the synthesis of epicuticular wax crystals on stem and hypocotyl surfaces of *Ricinus communis*. Arch. Biochem. Biophys. 448:60–72.

Hayashi, H., Sudo, H. (2007) Economic importance of licorice. Plant Biotechnol. 26:101–104.

Hayashi, H., Huang, P., Takada, S., Obinata, M., Inoue, K., Shibuya, M., Ebizuka, Y. (2004) Differential expression of three oxidosqualene cyclase mRNAs in *Glycyrrhiza glabra*. Biol. Pharm. Bull. 7:1986–1992.

Herrera, J.B.R., Bartel, B., Wilson, W.K., Matsuda, S.P.T. (1998) Cloning and characterization of the *Arabidopsis thaliana* lupeol synthase gene. Phytochemistry 49:1905–1977.

Iturbe-Ormaetxe, I., Haralampidis, K., Papadopoulou, K., Osbourn, A.E. (2003) Molecular cloning and characterization of triterpene synthases from *Medicago truncatula* and *Lotus japonicus*. Plant Mol. Biol. 51:731–743.

Jung, J.D., Park, H.W., Hahn, Y., Hur, C.G., In, D.S., Chung, H.J., Liu, J.R., Choi, D.W. (2003) Discovery of genes for ginsenoside biosynthesis by analysis of ginseng expressed sequence tags. Plant Cell Rep. 22:224–230.

Kenarova, B., Neychev, H., Hadjiivanova, C., Petkov, V.D. (1990) Immunomodulating activity of ginsenoside Rg1 from *Panax ginseng*. Jpn. J. Pharmacol. 54:447–454.

Kiem, P.V., Minh, C.V., Cai, X.F., Lee, J.J., Kim, Y.H. (2003) A new 24-nor-lupane-glycoside of *Acanthopanax trifoliatus*. Arch. Pharm. Res. 26:706–708.

Kuo, P.-M., Hsu, K.-H., Lee, Y.-R., Chu, F.-H., Wang, S.-Y. (2012) Isolation and characterization of β-cadinene synthase cDNA from *Chamaecyparis formosensis* Matsum. Holzforschung 66:569–576.

Kushiro, T., Shibuya, M., Masuda, K., Ebizuka, Y. (2000) Mutational studies on triterpene synthases: engineering lupeol synthase into β-amyrin synthase. J. Am. Chem. Soc. 122:6816–6824.

Liang, Y., Zhao, S. (2008) Progress in understanding of ginsenoside biosynthesis. Plant Biol. 10:415–421.

Liem, P.V., Cai, X.F., Minh, C.V., Lee, J.J., Kim, Y.H. (2003) Lupane-triterpene carboxylic acids from the leaves of *Acanthopanax trifoliatus*. Chem. Pharm. Bull. 51:1432–1435.

Lischewski, M., Ty, P.D., Kutschabsky, L., Pfeiffer, D., Phiet, H.V., Preiss, A., Sung, T.V., Adam, G. (1985) Two 24-nor-triterpenoid carboxylic acids from *Acanthopanax trifoliatus*. Phytochemistry 24:2355–2357.

McConn, M., Creelman, R.A., Bell, E., Mullet, J.E., Browse, J. (1997) Jasmonate is essential for insect defense in *Arabidopsis*. Proc. Natl. Acad. Sci. USA 94:5473–5477.

Mochizuki, M., Yoo, Y.C., Matsuzawa, K., Sato, K., Saiki, I., Tono-oka, S., Samukawa, K., Azuma, I. (1995) Inhibitory effect of tumor metastasis in mice by saponins, ginsenoside-Rb2,

20(R)- and 20(S)-ginsenoside-Rg3, of red ginseng. Biol. Pharm. Bull. 18:1197–1202.

Mylona, P., Owatworakit, A., Papadopoulou, K., Jenner, H., Qin, B., Findlay, K., Hill, L., Qi, X., Bakht, S., Melton, R., Osbourn, A. (2008) Sad3 and sad4 are required for saponin biosynthesis and root development in oat. Plant Cell 20:201–212.

Ohashi, H. (1993) Araliaceae. In: Flora of Taiwan. Eds. Huang, T.C. National Taiwan University, Taipei. pp. 986–1009.

Pauwels, L., Inzé, D., Goossens, A. (2009) Jasmonate-inducible gene: what does it mean? Trends Plant Sci. 14:87–91.

Pettersen, E.F., Goddard, T.D., Huang, C.C., Couch, G.S., Greenblatt, D.M., Meng, E.C., Ferrin, T.E. (2004) UCSF Chimera – a visualization system for exploratory research and analysis. J. Comput. Chem. 25:1605–1612.

Phillips, D.R., Rasbery, J.M., Bartel, B., Matsuda, S.P.T. (2006) Biosynthetic diversity in plant triterpene cyclization. Curr. Opin. Plant Biol. 9:305–314.

Prasad, S., Nigam, N., Kalra, N., Shukla, Y. (2008) Regulation of signaling pathways involved in lupeol induced inhibition of proliferation and induction of apoptosis in human prostate cancer cells. Mol. Carcinog. 47:916–924.

Reddy, K.P., Singh, A.B., Puri, A., Srivastava, A.K., Narender, T. (2009) Synthesis of novel triterpenoid (lupeol) derivatives and their in vivo antihyperglycemic and antidyslipidemic activity. Bioorg. Med. Chem. Lett. 19:4463–4466.

Saleem, M., Afaq, F., Adhami, V.M., Mukhtar, H. (2004) Lupeol modulates NF-jB and PI3K/Akt pathways and inhibits skin cancer in CD-1 mice. Oncogene 23:5203–5214.

Segura, M.J.R., Jackson, B.E., Matsuda, S.P.T. (2003) Mutagenesis approaches to deduce structure-function relationship in terpene synthases. Nat. Prod. Rep. 20:304–317.

Seo, J.W., Jeong, J.H., Shin, C.G., Lo, S.C., Han, S.S., Yu, K.W., Harada, E., Han, J.Y., Choi, Y.E. (2005) Overexpression of squalene synthase in *Eleutherococcus senticosus* increases phytosterol and triterpene accumulation. Phytochemistry 66:869–877.

Shinkai, K., Akedo, H., Mukai, M., Imamura, F., Isoai, A., Kobayashi, M., Kitagawa, I. (1996) Inhibition of in vitro tumor cell invasion by ginsenoside Rg3. Cancer Sci. 87:357–362.

Suzuki, H., Reddy, M.S., Naoukina, M., Aziz, N., May, G.D., Huhman, D.V., Sumner, L.W., Blount, J.W., Mendes, P., Dixon, R.A. (2005) Methyl jasmonate and yeast elicitor induce differential transcriptional and metabolic re-programming in cell suspension cultures of the model legume *Medicago truncatula*. Planta 220:696–707.

Thaler, J.S., Owen, B., Higgins, V.J. (2004) The role of the jasmonate response in plant susceptibility to diverse pathogens with a range of lifestyles. Plant Physiol. 135:530–538.

Thoma, R., Schulz-Gasch, T., D'Arcy, B., Benz, J., Aebi, J., Dehmlow, H., Hennig, M., Stihle, M., Ru, A. (2004) Insight into steroid scaffold formation from the structure of human oxidosqualene cyclase. Nature 432:118–122.

Trapp, S.C., Croteau, R.B. (2001) Genomic organization of plant terpene synthases and molecular evolutionary implications. Genetics 158:811–832.

Ty, P.D., Lischewski, M., Phiet, H.V., Sung, T.V., Schmidt, J., Adam, G. (1984) Two triterpenoid carboxylic from *Acanthopanax trifoliatus*. Phyochemistry 23:2889–2891.

Ty, P.D., Lischewski, M., Phiet, H.V., Preiss, A., Nguyen, P.V., Adam, G. (1985) 3α,11α-Dihydroxy-23-oxo-lup-20(29)-en-28-oic acid from *Acanthopanax trifoliatus*. Phytochemistry 24: 867–869.

Wen, J., Plunkett, G.M., Mitchell, A.D., Wagstaff, S.J. (2001) The evolution of Araliaceae: a phylogenetic analysis based on ITS sequences of nuclear ribosomal DNA. Syst. Bot. 26:144–167.

Wen, C.-H., Tseng, Y.-H., Chu, F.-H. (2012) Identification and functional characterization of a sesquiterpene synthase gene from *Eleutherococcus trifoliatus*. Holzforschung 66:183–189.

Wendt, K.U., Lenhart, A., Schulz, G.E., Feil, C., Poralla, K. (1997) Crystallization and preliminary X-ray crystallographic analysis of squalene-hopene cyclase from *Alicyclobacillus acidocaldarius*. Protein Sci. 6:722–724.

Xu, R., Fazio, G.C., Matsuda, S.P.T. (2004) On the origins of triterpenoid skeletal diversity. Phytochemistry 65:261–291.

Yook, C.S., Chang, S.Y., Lai, J.H., Ko, S.K., Jeong, J.H., Nohara, T. (1999) Lupane-glycoside of *Acanthopanax trifoliatus* forma *tristigmatis* leaves. Arch. Pharm. Res. 22:629–632.

You, Y.J., Nam, N.H., Kim, Y., Bae, K.H., Ahn, B.Z. (2003) Antiangiogenic activity of lupeol from *Bombax ceiba*. Phytother. Res. 17:341–344.